Published in final edited form as:
Science. 2013 July 26; 341(6144): . doi:10.1126/science.1238036.

Identification of a Colonial Chordate Histocompatibility Gene

Ayelet Voskoboynik[1,2,*,‡], **Aaron M. Newman**[1,*,‡], **Daniel M. Corey**[1], **Debashis Sahoo**[1], **Dmitry Pushkarev**[3,†], **Norma F. Neff**[3], **Benedetto Passarelli**[3], **Winston Koh**[3], **Katherine J. Ishizuka**[1,2], **Karla J. Palmeri**[1,2], **Ivan K. Dimov**[1], **Chen Keasar**[4], **H. Christina Fan**[3], **Gary L. Mantalas**[3], **Rahul Sinha**[1], **Lolita Penland**[3], **Stephen R. Quake**[3,‡], and **Irving L. Weissman**[1,2,5,‡]

[1]Institute for Stem Cell Biology and Regenerative Medicine, Stanford University School of Medicine, Stanford, CA 94305, USA

[2]Department of Developmental Biology, Stanford University, Hopkins Marine Station, Pacific Grove, CA 93950, USA

[3]Departments of Applied Physics and Bioengineering, Stanford University, and Howard Hughes Medical Institute, Stanford, CA 94305, USA

[4]Department of Computer Science, Ben-Gurion University of the Negev, Beer-Sheva 84105, Israel

[5]Ludwig Center for Cancer Stem Cell Research and Medicine, Stanford University School of Medicine, Stanford, CA 94305, USA

Abstract

Histocompatibility is the basis by which multicellular organisms of the same species distinguish self from non-self. Relatively little is known about the mechanisms underlying histocompatibility reactions in lower organisms. *Botryllus schlosseri* is a colonial urochordate, a sister group of vertebrates, that exhibits a genetically determined natural transplantation reaction, whereby self-recognition between colonies leads to formation of parabionts with a common vasculature, whereas rejection occurs between incompatible colonies. Using genetically defined lines, whole-transcriptome sequencing, and genomics, we identified a single gene that encodes self/non-self and determines "graft" outcomes in this organism. This gene is significantly upregulated in colonies poised to undergo fusion or rejection, is highly expressed in the vasculature, and is functionally linked to histocompatibility outcomes. These findings establish a platform for advancing the science of allorecognition.

Allorecognition, the capacity to distinguish "self" from allogeneic "nonself", is critical for multicellular life. This process also has important implications for humans, as it underlies maternal tolerance of the fetus (1–2) and the outcomes of blood or tissue transplants (3–4). To gain insights into the evolution and molecular characteristics of allorecognition, we are

‡Corresponding authors: ayeletv@stanford.edu (A.V.), amnewman@stanford.edu (A.M.N.), quake@stanford.edu (S.R.Q.), irv@stanford.edu (I.L.W.).
*These authors contributed equally to this work.
†Present address: Illumina Inc., Hayward, CA 94545, USA.

Supplementary Materials
www.sciencemag.org
Materials and Methods
Figs. S1 to S21
Tables S1 to S9
Movies S1 and S2
References (26–42)

studying *Botryllus schlosseri*, a member of the urochordates, the closest living sister group of vertebrates (5). *B. schlosseri* engages in a natural transplantation reaction, whereby colonies undergo self-nonself recognition, which leads to either formation of parabionts with a fused vasculature (i.e., *fusion*) or an inflammatory rejection response (i.e., *rejection*) (fig. S1). A polymorphic gene locus governs fusion/rejection outcomes (6–9). This locus, called Fu/HC for fusion/histocompatibility, encodes multiple co-dominant alleles, and progeny from crosses between histocompatible *B. schlosseri* colonies are known to segregate as a monogenic trait (8, 9). The rules governing fusibility reactions are as follows: AB=AB leads to fusion, AB=CD to rejection, and AB=BC to fusion. Previously, we identified a highly polymorphic candidate allorecognition gene (*cFuHC*) within the Fu/HC locus (10–12). As the major histocompatibility regions in vertebrates are haplotypes (that is, sets of linked genes), we analyzed the recently completed *B. schlosseri* genome (13) to determine whether a haplotype or single protein-encoding gene encodes self-nonself recognition.

Using diverse sequencing data, we first attempted to validate the genomic structure of the *cFuHC*, which previously appeared to correlate with fusion or rejection outcomes (12). The original *cFuHC* model consists of two dominant isoforms, a secreted form and a membrane-bound form encompassing the entire predicted gene (12). We found that instead of two isoforms, the *cFuHC* consists of two genes separated by 250 base pairs (bp) (Fig. 1, tables S1–S3). We found no evidence for an mRNA isoform bridging these two genes (table S4). One gene, which we term *sFuHC*, is identical to the original secreted isoform; the other, termed *mFuHC*, includes the remaining portion of *cFuHC*, but has a novel N-terminal exon encoding a signal peptide (14) (table S5). BLAST analysis revealed a homolog of *mFuHC*, but not *sFuHC*, in *Ciona intestinalis* (gi|198429243) [Expectation value (E-value) = $4e^{-37}$], which further supported our finding. Both genes are highly polymorphic (fig. S2), as previously reported for *cFuHC* (12).

Next, we tested whether any genes from the draft assembly encode alleles consistent with a *Botryllus* histocompatibility factor. We used two complementary strategies, one to assess allelic concordance with known fusibility outcomes and the other to evaluate allelic agreement with Fu/HC genotypes defined by breeding experiments. For the former, we developed a computational pipeline that includes methods to accurately and efficiently phase paired-end RNA sequencing (RNA-Seq) reads into haplotypes, compare phased alleles between colonies, and score each gene based on its ability to stratify known fusibility outcomes (figs. S3 to S7; 15). For the latter, we established lines of distinct Fu/HC genotypes (AA, BB, AB and AX), and used a classical genetics approach (fig. S8). By performing RNA-Seq on colonies with defined Fu/HC genotypes (fig. S8), we could precisely screen for allorecognition factor candidates, because any genes inconsistent with defined genotypes must be incorrect.

In all, 17 colonies encompassing 29 pairs of known fusion-rejection outcomes were analyzed. To increase sensitivity, we included pairs of related rejecting colonies bred in our laboratory and unrelated fusing colonies obtained from the wild (fig S8). Transcriptome sequencing (table S4), followed by haplotype phasing and interallele comparison (fig. S4), revealed that *sFuHC* and, to some extent, *mFuHC*, significantly stratify colony pairs by known fusion-rejection outcomes (P≈5.6×10^{-5} and P≈0.05, respectively, as determined by 1 million random permutations of known fusion-rejection labels across the genome) (Fig. 2A and tables S5 and S6). Although significant, segregation was not perfect for either gene (Fig. 2A and fig. S9), and neither *sFuHC* nor *mFuHC* are concordant in primary sequence among all AA colonies (fig. S9), and so, they fail the classical genetics test. These results indicate that the allorecognition factor in *B. schlosseri* is encoded by another gene, consistent with a recent report (16).

Our unbiased genome-wide scan revealed three candidate genes with perfect classification performance (Fig. 2A). Among them, only one gene is also fully consistent with genetically defined lines (Fig. 2B; Database S2 and table S6). This gene is free of any amino acid differences between histocompatible pairs (Fig. 2B); is highly polymorphic (Fig. 2C); and, on the basis of RNA-Seq, is expressed more highly than either *sFuHC* or *mFuHC* (fig. S10). It is striking that analysis of the fosmid sequence used to identify *cFuHC* revealed that this gene is located ~62kb away from *sFuHC* and *mFuHC* (Fig. 2C and table S5). Analysis of the draft genome confirmed physical linkage for these three genes (13).

We termed this candidate Fu/HC gene, "*Botryllus* Histocompatibility Factor" (*BHF*), and further analyzed its sequence, relationship to fusibility outcomes, and expression patterns. *BHF* is composed of three exons, encoding a highly charged and partially unstructured 252-amino acid protein (Fig. 2C, fig. S11, and tables S5 and S7), with no detectable domains or signal peptide (14). BHF has three remote homologs in the National Center for Biotechnology Information (NCBI) database, all of which encode uncharacterized proteins from solitary tunicates (fig. S12). Because colonial but not solitary tunicates participate in fusibility reactions, we attempted to amplify BHF from two other colonial tunicate species (*Botrylloides* sp. and *Diplosoma* sp.). We succeeded in recovering highly similar sequences from both species (fig. S12), which indicated that BHF may represent a general colonial tunicate allorecognition actor. To validate *BHF*, we sequenced four additional *B. schlosseri* colonies by RNA-Seq (Fig. 3A and table S4), and performed *BHF* Sanger-sequencing on two additional AA colonies (fig. S13). We found that *BHF* absolutely aligns with fusibility outcomes in the validation cohort (Fig. 3A), and is homozygous and identical in sequence among all AA colonies (fig. S14A). Moreover, polymorphisms within the first 100 amino acids could predict the outcomes of all histocompatibility reactions (fig. S14B), and at the nucleotide level, BHF remains absolutely predictive (fig. S15).

Among the 23 colonies examined, we determined 10 unique *BHF* alleles that not only agree with all known fusibility outcomes (Fig. 3A and fig. S14) and known pedigree relations (fig. S13), but also allow for the confirmation of precise predictions of *B. schlosseri* self-non-self recognition events. As an example, we predicted that colony 31 (genotype AD) would fuse with colony 944 (genotype AD) and reject colony 4 (genotype BI), and that colony Sc109e would fuse with colony 31. Indeed, we confirmed our predictions for these pairs, along with all other pairs tested (n=6 of 6) (Fig. 3A and, e.g., fig. S16).

We next asked whether *BHF* is up-regulated under the conditions preceding fusion or rejection, a potential outcome of a bona fide fusibility factor. In tissues that participate in allorecognition (vasculature/tunic), levels of *BHF*, *sFuHC*, and *mFuHC* were assessed by real-time polymerase chain reaction (PCR) in both apposing colonies ("challenged") and physically unpaired colonies ("naïve"). We found a significant upregulation of *BHF* but not *sFuHC* or *mFuHC* in challenged colonies (two-tailed t test, P=0.009) (Fig. 3B). Moreover, among these three genes, only *BHF* was found among transcripts associated with the *B. schlosseri* rejection response (17) (table S6).

We next investigated *BHF* localization and expression. Using whole-mount *in situ* hybridization, we found high expression levels of *BHF* in blood vessels, including cells in the ampullae (Fig. 3C, top). Increased *BHF* expression was also observed on cells lining the periphery of blood vessels, consistent with epithelium (Fig. 3C, bottom). By RNA-Seq, we found enriched expression of *BHF* in the vasculature compared to endostyle (fig. S17), and by semi-quantitative PCR and Sanger-sequencing, we found broad expression of *BHF* in blood, ampullae, bud, endostyle region, tadpole, and sperm (fig. S18). These data are consistent with a histocompatibility-related function for BHF.

Finally, to assess BHF function, we performed morpholino-mediated knockdown experiments (15). In colony allorecognition assays, three of four isogenic pairs receiving control morpholinos fused within 24 hours of ampullae contact. By contrast, no reactions were observed in isogenic pairs receiving BHF translation-blocking morpholinos (n=6), despite constant physical contact over observational periods ranging from 2 to 7 days (Fig. 3D, fig. S19, and table S8). To exclude nonspecific effects, we also tested *BHF* splice-inhibiting morpholinos, using the progeny of wild-type colonies (15). Within 2 days of ampullae contact, all control pairs had fused (n=2) or rejected (n=1), whereas colony pairs receiving splice-inhibiting morpholinos did not react (n=5) (figs. S20 and S21, table S9, and movies S1 and S2). These data support our genomic analysis and indicate that BHF participates in fusion and rejection initiation.

In the jawed vertebrates the MHC is a haplotype, each sublocus of which specifies a different recognition process, usually by unique subsets of cells (18–20). By contrast, the *B. schlosseri* Fu/HC locus is a single gene (BHF) embedded in a haplotype of several genes with high polymorphism. Unlike the secreted (*sFuHC*) and membrane-bound (*mFuHC*) genes, *BHF* has none of the domains expected for a cell surface recognition protein or, in fact, domains that are conserved throughout protein evolution. Because *BHF* does not follow biological precedence by either sequence or domains, future investigations of this gene will likely reveal new mechanisms of recognition.

The ability to reliably predict histocompatibility outcomes on the basis of a single gene has broad implications for the study of allorecognition. For example, after vasculature fusion, stem cells from each *B. schlosseri* colony compete to overtake germline and/or somatic lineages (21–24). Stem cell competition may lead to elimination the other colony's genome, or may produce a chimeric colony with mixed genotypes. To date, induction of chimerism using hematopoietic stem-cell transplantation is the only way to achieve long-term donor-specific tolerance to human organ allografts (25). Chimerism can be short-lived, and if lost, the threat of allograft rejection emerges. *B. schlosseri* is a unique species for studying stem cell-mediated chimerism, and such research will be facilitated by BHF.

Supplementary Material

Refer to Web version on PubMed Central for supplementary material.

Acknowledgments

We thank B. Rinkevich for pointing out the difficulty with the original cFuHC assignments, T. Snyder, J. Okamoto, L. Me, L. Ooi, A. Dominguez, C. Lowe, K. Uhlinger, L. Crowder, S. Karten, C. Patton, L. Jerabek, and T. Storm for invaluable technical advice and help. A. De Tomaso provided the fosmid sequence used to characterize *cFuHC* (12) (table s5). D.P., A.V., and S.R.Q. have filed U.S. and international patent applications (61/532,882 and 13/608,778, respectively) entitled "Methods for obtaining a sequence." This invention allows for the sequencing of long continuous (kilobase scale) nucleic acid fragments using conventional short read–sequencing technologies, useful for consensus sequencing and haplotype determination. This study was supported by National Institutes of Health (NIH) grants 1R56AI089968, RO1GM100315 and 1R01AG037968 awarded to I.L.W, A.V., and S.R.Q., respectively, and the Virginia and D.K. Ludwig Fund for Cancer Research awarded to I.L.W. D.S. was supported by NIH Grant K99CA151673-01A1 and Department of Defense Grant W81XWH-10-1-0500, and A.M.N., D.M.C., D.S., and I.K.D. were supported by a grant from the Siebel Stem Cell Institute and the Thomas and Stacey Siebel Foundation. The data in this paper are tabulated in the main manuscript and in the supplementary materials. BHF, sFuHC, and mFuHC sequences are available in GenBank under accession numbers KF017887-KF017889, and the RNA-Seq data are available on the Sequence Read Archive (SRA) database: BioProject SRP022042.

References and Notes

1. Nakashima A, Shima T, Inada K, Ito M, Saito S. The balance of the immune system between T cells and NK cells in miscarriage. Am J Reprod Immunol. 2012; 67:304–10. [PubMed: 22364212]

2. Girardi G, Prohászka Z, Bulla R, Tedesco F, Scherjon S. Complement activation in animal and human pregnancies as a model for immunological recognition. Mol Immunol. 2011; 48:1621–30. [PubMed: 21600656]
3. Colonna M, Jonjic S, Watzl C. Natural killer cells: fighting viruses and much more. Nature Immunology. 2011; 12:107–10. [PubMed: 21245897]
4. LaRosa DF, Rahman AH, Turka LA. The innate immune system in allograft rejection and tolerance. J Immunol. 2007; 178:7503–9. [PubMed: 17548582]
5. Delsuc F, Brinkmann H, Chourrout D, Philippe H. Tunicates and not cephalochordates are the closest living relatives of vertebrates. Nature. 2006; 439:965–968. [PubMed: 16495997]
6. Oka H, Watanabe H. Colony specificity in compound ascidians as tested by fusion experiments (a preliminary report). Proc Jpn Acad. 1957; 33:657–659.
7. Oka H, Watanabe H. Problems of colony specificity in compound ascidians. Bull Mar Biol Stat Asamushi. 1960; 10:153–155.
8. Sabbadin A. Le basi geneticha della capacita di fusion fra colonies in *B. schlosseri* (Ascidiacea). Rend Accad Naz Lincei Ser. 1962; 32:1031–1035.
9. Scofield VL, Schlumpberger JM, West LA, Weissman IL. Protochordate allorecognition is controlled by a MHC-like gene system. Nature. 1982; 295:499–502. [PubMed: 7057909]
10. De Tomaso AW, Saito Y, Ishizuka KJ, Palmeri KJ, Weissman IL. Mapping the genome of a model protochordate. I. A low resolution genetic map encompassing the fusion/histocompatibility (Fu/HC) locus of *B. schlosseri*. Genetics. 1998; 149:277–287. [PubMed: 9584102]
11. De Tomaso AW, Weissman IL. Initial characterization of a protochordate histocompatibility locus. Immunogenetics. 2003; 55:480–490. [PubMed: 14520503]
12. De Tomaso AW, et al. Isolation and characterization of a protochordate histocompatibility locus. Nature. 2005; 438:454–459. [PubMed: 16306984]
13. Voskoboynik A, et al. The *Botryllus schlosseri* genome: a genetic toolkit for the investigation of regeneration and immune system evolution. eLIFE. 2013; 2:e00569. [PubMed: 23840927]
14. Letunic I, Doerks T, Bork P. SMART 7: recent updates to the protein domain annotation resource. Nucleic Acids Res. 2012; 40:D302–D305. [PubMed: 22053084]
15. Materials and methods are available as supplementary material on *Science* Online.
16. Rinkevich B, Douek J, Rabinowitz C, Paz G. The candidate FuHC gene in *B. schlosseri* (Urochordata) and ascidians' historecognition – An oxymoron? Dev Comp Immunol. 2012; 36:718–72. [PubMed: 22085780]
17. Oren M, Douek J, Fishelson Z, Rinkevich B. Identification of immune-relevant genes in histocompatible rejecting colonies of the tunicate *Botryllus schlosseri*. Dev Comp Immunol. 2007; 31:889–902. [PubMed: 17287019]
18. The MHC sequencing consortium. Complete sequence and gene map of human major histocompatibility complex. Nature. 1999; 401:921–923. [PubMed: 10553908]
19. Hirano M, Das S, Guo P, Cooper MD. Chapter 4 – The evolution of adaptive immunity in vertebrate. Adv In Immunol. 2011; 109:125–157. [PubMed: 21569914]
20. Dishaw LJ, Litman GW. Invertebrate Allorecognition: The origins of histocompatibility. Current Biol. 2009; 19:R286–R288.
21. Stoner DS, Weissman IL. Somatic and germ cell parasitism in a colonial ascidian: possible role for a highly polymorphic allorecognition system. Proc Natl Acad Sci USA. 1996; 93:15254–15259. [PubMed: 8986797]
22. Stoner DS, Rinkevich B, Weissman IL. Heritable germ and somatic cell lineage competitions in chimeric colonial protochordates. Proc Natl Acad Sci USA. 1999; 96:9148–9153. [PubMed: 10430910]
23. Laird DJ, De Tomaso AW, Weissman IL. Stem cells are units of natural selection in a colonial ascidian. Cell. 2005; 123:1351–1360. [PubMed: 16377573]
24. Voskoboynik A, et al. Identification of the endostyle as a stem cell niche in a colonial chordate. Cell Stem Cell. 2008; 3:456–464. [PubMed: 18940736]

25. Sachs DH, Sykes M, Kawai T, Cosimi AB. Immuno-intervention for the induction of transplantation tolerance through mixed chimerism. Semin Immunol. 2011; 23:165–173. [PubMed: 21839648]
26. Boyd HC, Brown SK, Harp JA, Weissman IL. Growth and sexual maturation of laboratory-cultured Monterey *B. schlosseri*. Biol Bull. 1986; 170:91–109.
27. Zerbino DR. Using the Velvet de novo assembler for short-read sequencing technologies. Curr Protoc Bioinformatics. 2010; 11:11.5.1–11.5.12.
28. Myers EW, et al. A Whole-Genome Assembly of Drosophila. Science. 2000; 287:2196–2204. [PubMed: 10731133]
29. Fan HC, et al. Whole-genome molecular haplotyping of single cells. Nat Biotechnol. 2011; 29:51–57. [PubMed: 21170043]
30. Xu X, et al. The genomic sequence of the Chinese hamster ovary (CHO)-K1 cell line. Nat Biotechnol. 2011; 29:735–741. [PubMed: 21804562]
31. Li H, Durbin R. Fast and accurate short read alignment with Burrows-Wheeler Transform. Bioinformatics. 2009; 25:1754–1760. [PubMed: 19451168]
32. Trapnell C, et al. Transcript assembly and quantification by RNA-Seq reveals unannotated transcripts and isoform switching during cell differentiation. Nat Biotechnol. 2010; 28:511–515. [PubMed: 20436464]
33. Stanke M, Diekhans M, Baertsch R, Haussler D. Using native and syntenically mapped cDNA alignments to improve *de novo* gene finding. Bioinformatics. 2008; 24:637–644. [PubMed: 18218656]
34. Lowe CJ, et al. Hemichordate embryos: procurement, culture and basic methods. Methods Cell Biol. 2004; 74:171–194. [PubMed: 15575607]
35. Eisen JS, Smith JC. Controlling morpholino experiments: don't stop making antisense. Development. 2008; 135:1735–1743. [PubMed: 18403413]
36. Koboldt DC, et al. VarScan 2: somatic mutation and copy number alteration discovery in cancer by exome sequencing. Genome Res. 2012; 22:568–576. [PubMed: 22300766]
37. Tamura K, et al. MEGA5: Molecular Evolutionary Genetics Analysis using Maximum Likelihood, Evolutionary Distance, and Maximum Parsimony Methods. Mol Biol Evol. 2011; 28:2731–2739. [PubMed: 21546353]
38. Rossi P, et al. A microscale protein NMR sample screening pipeline. J Biomol NMR. 2010; 46:11–22. [PubMed: 19915800]
39. Edgar RC. MUSCLE: multiple sequence alignment with high accuracy and high throughput. Nucl Acids Res. 2004; 32:1792–1797. [PubMed: 15034147]
40. Waterhouse AM, et al. Jalview version 2: A Multiple Sequence Alignment and Analysis Workbench. Bioinformatics. 2009; 25:1189–1191. [PubMed: 19151095]
41. Clamp M, et al. The Jalview Java Alignment Editor. Bioinformatics. 2004; 20:426–427. [PubMed: 14960472]
42. Li H, et al. The Sequence Alignment Map format and SAM tools. Bioinformatics. 2009; 25:2078–2079. [PubMed: 19505943]

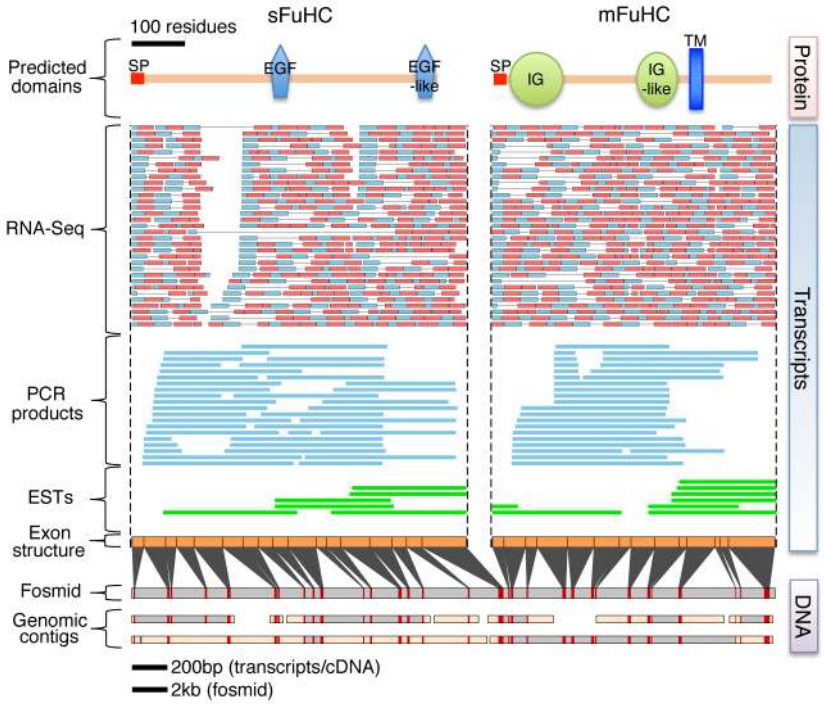

Fig. 1. Genomic characterization of the *cFuHC* locus in *B. schlosseri* reveals two tightly linked genes

The *cFuHC* locus encodes two gene products, sFuHC (a secreted form) and mFuHC (a membrane-bound form). Sequences aligned, from bottom to top: (i) Genomic contigs from *B. schlosseri* draft assembly; (ii) Fosmid clone used to characterize *cFuHC* (12) (table S5); (iii) predicted exon structures, with genomic coordinates indicated below in red (contigs with identical interexon distances to the fosmid are colored gray); (iv) *B. schlosseri* expressed sequence tags (ESTs) obtained from NCBI; (v) Sanger-sequenced PCR products resulting from selected c*FuHC* amplicons (table S1); (vi) representative RNA-Seq reads (100 bp × 2) from 17 colonies (table S4); (vii) translated primary sequences with predicted functional domains (14). All alignments were performed with megablast (mismatch penalty = −2, ≥90% identity, no query filtering, and otherwise default parameters). EGF, epidermal growth factor; IG, immunoglobulin domain; SP, signal peptide; TM, transmembrane domain.

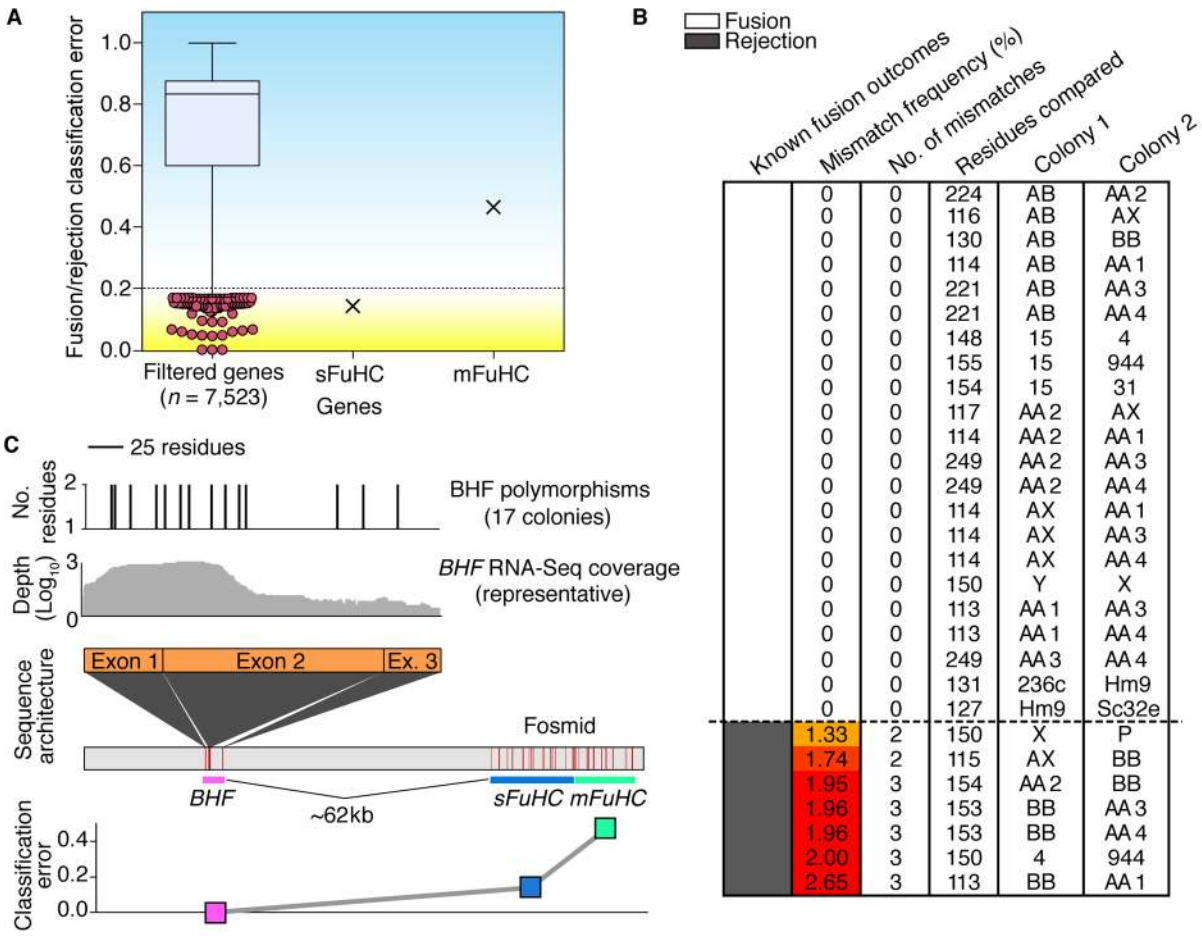

Fig. 2. Genome-wide analysis for candidate Fu/HCs reveals a single gene that exhibits perfect alignment with fusibility outcomes and defined Fu/HC genotypes

The ability to stratify known fusion or rejection outcomes was tested for all predicted genes from the draft assembly having transcriptome data covering ≥6 fusion and ≥6 rejection pairs, ≥20 common sites sequenced per pair, and at least 1 amino acid polymorphism (after filtering, $n = 7,523$ genes) (table S5). **A**, Classification errors across the genome are depicted as a boxplot showing the median (horizontal line), 25th to 75th percentiles (within the box), and 1st to 99th percentiles (whiskers). Although *sFuHC* is in the top 1% of best-performing genes, novel Fu/HC candidates with equal or better performance were also identified and are indicated in pink beneath the boxplot. Classification errors <0.2 (dotted line) have a p-value < 0.001, as determined by 1 million random permutations of known fusibility outcomes for each gene analyzed in the assembly (table S6). **B**, A *B. schlosseri* gene that exhibits perfect sequence concordance with fusion or rejection outcomes and defined genotypes, termed *BHF*. **C**, *BHF* genomic and message sequence architecture (table S7), representative RNA-Seq coverage and amino acid polymorphisms across all 17 colonies from the exploratory cohort (tables S4).

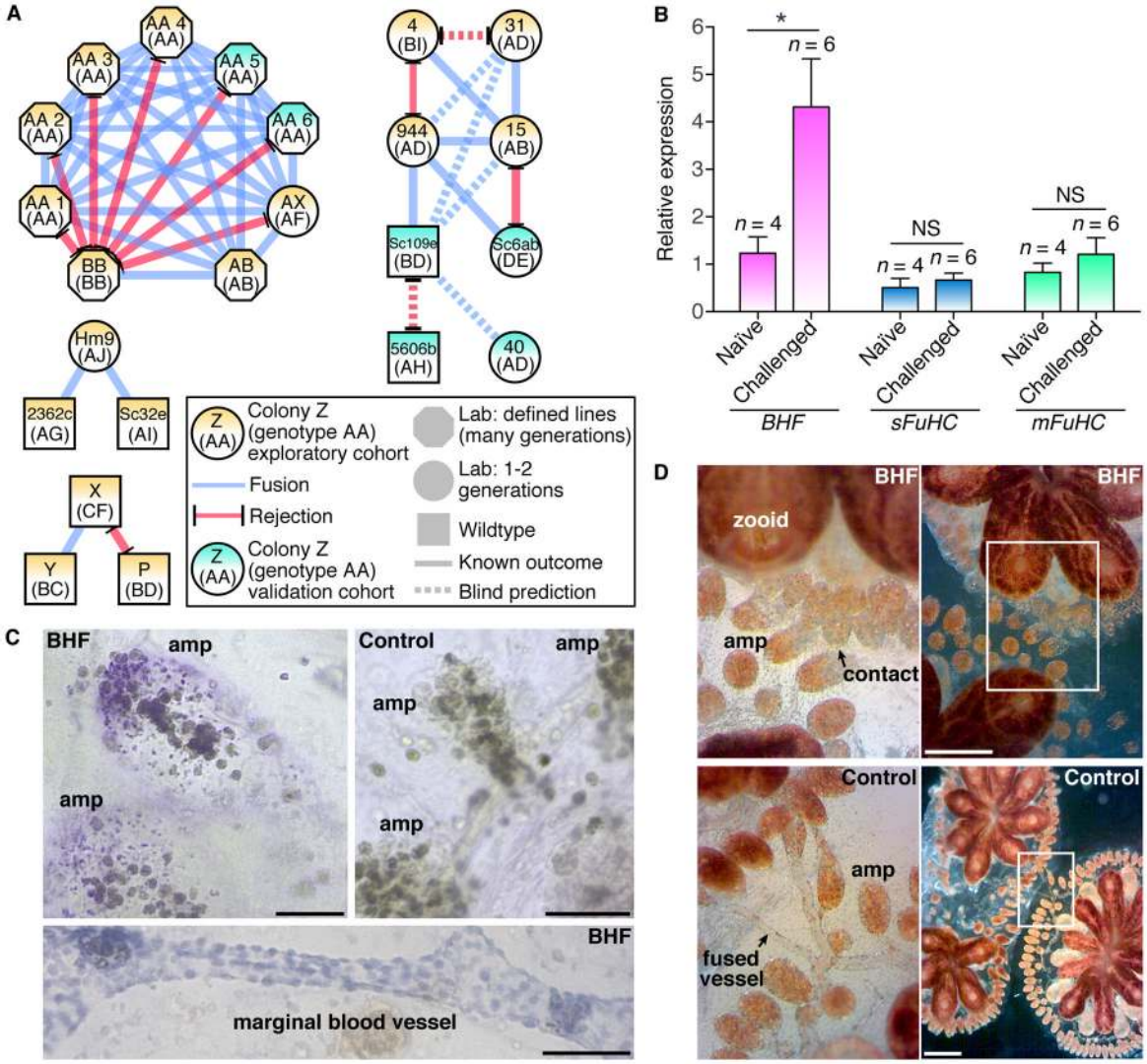

Fig. 3. BHF accurately predicts new fusibility outcomes and has expression patterns and function consistent with a *Botryllus* allorecognition determinant

A, Known and predicted fusion or rejection outcomes among all 23 *B. schlosseri* colonies analyzed (table S4), including exploratory ($n = 17$) and validation cohorts ($n = 6$). All "blind" predictions were confirmed (6 of 6). **B**, Expression analysis of *BHF*, *sFuHC*, and *mFuHC* under the conditions preceding fusion or rejection ("challenged"; $n = 6$) compared to unchallenged control colonies ("naïve"; $n = 4$) ($^*P = 0.009$, two-tailed unequal variance *t* test; NS, not significant). Values are presented as mean +/−SEM. **C**, *BHF* expression patterns assessed by whole-mount in situ hybridization, compared with control (sense probe). amp, ampullae. Scale bars, 50 □m. **D**, Analysis of morpholino-induced knockdown of BHF. Top: Unreactive ampullae from apposing colonies under BHF-knockdown conditions (left) and at lower magnification (right). (Bottom) Fused blood vessels between colonies injected with morpholino control (left) and at lower magnification (right). amp, ampullae. Scale bars, 1mm.